Journal Pre-proof

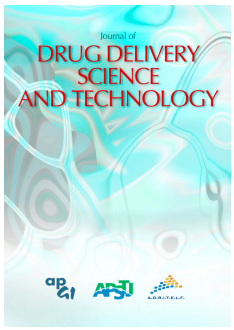

GELATIN/CELLULOSE nanowhiskers hydrogels intended for the administration of drugs in dental treatments: Study of lidocaine as model case

F. Favatela, M.F. Horst, M. Bracone, J. Gonzalez, V. Alvarez, V. Lassalle

PII: S1773-2247(20)31175-8

DOI: https://doi.org/10.1016/j.jddst.2020.101886

Reference: JDDST 101886

To appear in: *Journal of Drug Delivery Science and Technology*

Received Date: 17 July 2019

Revised Date: 27 May 2020

Accepted Date: 18 June 2020

Please cite this article as: F. Favatela, M.F. Horst, M. Bracone, J. Gonzalez, V Alvarez, V Lassalle, GELATIN/CELLULOSE nanowhiskers hydrogels intended for the administration of drugs in dental treatments: Study of lidocaine as model case, *Journal of Drug Delivery Science and Technology*, https://doi.org/10.1016/j.jddst.2020.101886.

This is a PDF file of an article that has undergone enhancements after acceptance, such as the addition of a cover page and metadata, and formatting for readability, but it is not yet the definitive version of record. This version will undergo additional copyediting, typesetting and review before it is published in its final form, but we are providing this version to give early visibility of the article. Please note that, during the production process, errors may be discovered which could affect the content, and all legal disclaimers that apply to the journal pertain.

© 2020 Elsevier B.V. All rights reserved.

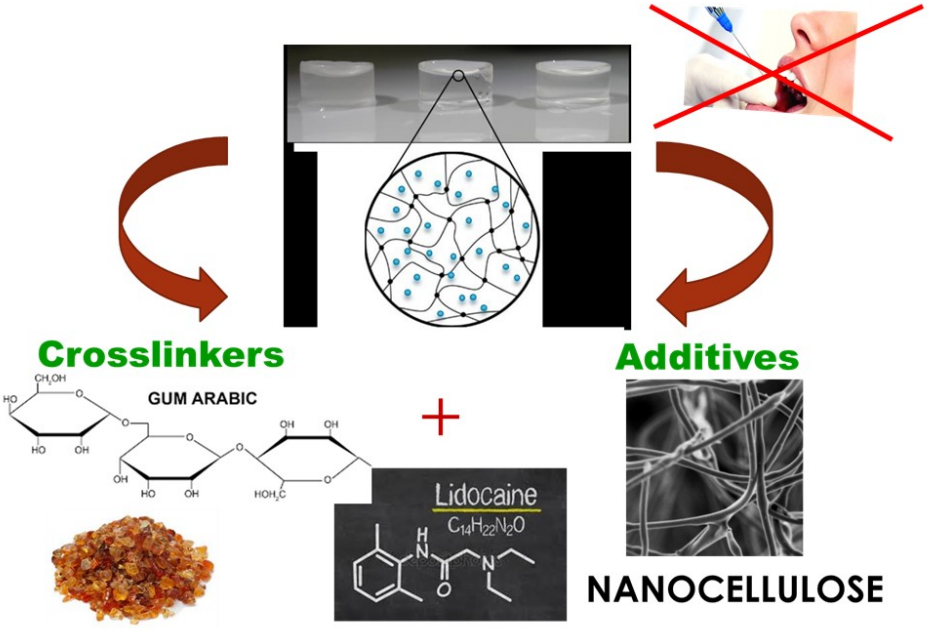
Crosslinkers
GUM ARABIC
Lidocaine
$C_{14}H_{22}N_2O$
Additives
NANOCELLULOSE

Journal Pre

Journal Pre-proof

Author statement

Florencia Favatela: Experimental work: Synthesis of gels, assays related to Gel fraction, solubility and swelling. Collection of data of UV-visible and FTIR.

Fernanda Horst: Synthesis of gels loaded lidocaine and SEM and rheology characterization.

Melina Brancone: Preparation of nanocellulose whiskers and characterization of them.

Jimena Gonzalez: Characterization of nanocellulose whiskers and thermal characterization of gels.

Vera Alvarez: Discussion of data. Writing- Reviewing and Editing

Verónica Lassalle: Propose and organize the research topic concerning the article. Analysis of drug loading and release kinetic. Discussion of data. Writing- Original draft preparation. Writing- Reviewing and Editing.

Journal Pre-Proof

Journal Pre-proof

GELATIN/CELLULOSE NANOWHISKERS HYDROGELS INTENDED FOR THE ADMINISTRATION OF DRUGS IN DENTAL TREATMENTS: STUDY OF LIDOCAINE AS MODEL CASE

F. Favatela[1], M.F. Horst[1], M. Bracone[2], J. Gonzalez[2], V.Alvarez[2] and V.Lassalle[1]*

[1]INQUISUR-Departamento de Química-Universidad Nacional del Sur-CONICET, Avenida Alem 1253, 8000, Bahía Blanca, R. Argentina.

[2] Thermoplastic Composite Group (ComP), Institute of Materials Science and Technology (INTEMA), University of Mar del Plata and National Research Council (CONICET), Colón 10890, 7600 Mar del Plata, Argentine.

Journal Pre-proof

ABSTRACT

Gelatin based hydrogels were synthesized by the thawing- freezing method employing gum Arabic as crosslinking agent. The incorporation of cellulose nanowhiskers (NC) was analysed aiming to reach a control over the solubility/degradation rate, swelling properties and their ability to load anaesthetic drugs. Three concentrations of NC were explored, i.e: 1, 2 and 5%w/w with respect to the gelatin mass. The raw and NC containing hydrogels were well characterized in terms of the main properties regarding the intended application. Hence the swelling behaviour, solubility rate, gel fraction were determined as well as their thermal, morphological and rheological properties.

In this work, the obtained biocompatible hydrogels have tested for their potential application in the lidocaine administration during dental practices. This drug has been taken as model between other potential therapeutic agents for buccal treatments such as antibiotics, analgesics, etc. The kinetic and mechanism of LID release were studied by means of available mathematical models. The hydrogels loaded LID here presented would be considered as potential raw materials to the fabrication of buccal patches in order to avoid, or at least minimize, the extensive use of injected anaesthesia during dental treatments.

Journal Pre-proof

KEYWORDS: GELATIN, HYDROGELS, NANOCELLULOSE, LIDOCAINE, ANESTHESIA DRUG DELIVERY.

*Corresponding Author. Dra. Verónica Lassalle, INQUISUR, Alem 1253, Office 66J, 8000, Bahía Blanca, Bs.As.Argentina. veronica.lassalle@uns.edu.ar; velassalle@gmail.com.

INTRODUCTION

Biopolymers, such as gelatin and cellulose, have attracted special attention in multiple biomedical applications [1–3]. For instance A. Arbelaiz et al. developed bionanocomposite films based on a protein matrix reinforced with different nanocellulose systems (nanofibers and nanocrystals). This work was devoted to the structural and mechanical characterization of the prepared hydrogels without defining any application [2]. Wang and col. have studied the incorporation of cellulose nanofibers to gelatin gel, exploring different concentrations. The published article includes the morphology, mechanical, and sol-gel transversion characterization in view of the applications of these materials in food industry field [4]**.**

However, their application as dental patches to the administration of drugs in general and anaesthetics in particular has been hardly reported to the best of these author´s knowledge.

In local anaesthesia, drugs (local anaesthetics) that affect axonal impulse conduction are deposited at the desired site of action, interrupting the transmission of pain signals to the central nervous system. In dental treatments, these anaesthetics are normally applied by injection throughout the region of the mouth to be affected. The requirement of several doses is a common issue related to the most of dental treatments. Besides the pain and discomfort caused by these practices, other limitations are recognized. Between them incomplete anaesthesia doses, the occurrence of needle

Journal Pre-proof

phobia, the bleeding or hematoma formation and other serious systemic complications are frequently found [5]**.** Toward overcoming these limitations, pharmaceutical research is advancing in the formulation of novel devices that safely prolong and enhance the anaesthetic effect at the site of administration involving less invasive procedures [6]**.**

Numerous anaesthetics delivery systems have been developed in recent decades. Most of them are based on polymeric materials with capacity to bind to the drugs inducing a controlled release in the physiological conditions [7–11]**.** The use of multifunctional matrices, such as polyacrylates, cellulose derivatives, and chitosan, that display mucoadhesive properties, permeation-enhancing effects, enzyme-inhibiting properties, and/or a high buffer capacity, have proven successful strategies in oral drug delivery [12,13].

Lidocaine (LID) is a widely used medication for numbing tissue in a specific area and is commonly delivered as a subcutaneous or nerve targeting injection rather than other administrative dosages such as intravenous infusion and nasal spray. Its action mechanism involves the antagonism of nerve signals in cells by inhibiting the influx of sodium ions through the sodium channels of biological cell membranes resulting in a response to temporary pain blockage on the skin surface [14].

After a survey of available literature several examples of mucoadhesive patches, films and microparticles developed for the buccal delivery of lidocaine, may be found, [15–17].

The aim of this work is to study the synthesis of biodegradable hydrogels (HG) as efficient vehicles for the administration of drugs in buccal treatments, for instance by the design of dental patches. To this end, gelatin was chosen as polymeric matrix and gum Arabic (GA) as crosslinking agent. The HGs were prepared by the freeze thawing method, and variable concentrations of cellulose nanowiskers (NC) were incorporated to evaluate

Journal Pre-proof

their effect on the solubility, loaded of drug and degradation properties. Hence, structural and chemical characterization of the obtained hydrogel was performed.

Lidocaine (LID) was chosen as model drug and encapsulated on HG during the steps involved in the synthesis of the gels. The release behaviour was analysed in media simulated the buccal environment in order to determine the future perspectives of application of the designed biomaterials.

Although various in vitro investigations were carried out for the buccal formulations loaded with lidocaine, none of these studies focused on the use of the set of raw materials here proposed employing simple and fully biodegradable components and procedures.

This proposal provides useful perspectives for the implementation of a platform for the encapsulation and delivery of diverse therapeutic agents destined to buccal treatments.

EXPERIMENTAL

Materials

Gelatin 48723 tested according Ph. Eur (CAS Nº:9000-70-8) was purchased from Fluka Analytical. gum Arabic (GA) was provided by Biopack (Argentina). Commercial microcrystalline cellulose (MCC) was from Sigma Aldrich (USA). Hydrochloride lidocaine was from Anhedra (Argentina). Distilled water was used for the preparation of all reactant solutions. Buffer phosphate solution were prepared from potassium phosphate monobasic anhydrous from Biopack and potassium phosphate dibasic anhydrous from Anedra.

Synthesis methodology

Celullose nanowiskers preparation

Journal Pre-proof

Journal Pre-proof

Commercial micro-crystalline cellulose (CMF) from Sigma Aldrich (USA). The complete characterization of CMF was performed in a previous work[18]. Distilled water was used to prepare the suspensions. All reagents used were analytical grade.

Equipment

Ultrasonic Processor: Sonics model Vibra-cell VCX750; power 750W; frequency 20kHz. Probe: Standard for VCX750; tip model 219-B (630-0219); tip diameter 13 mm.

CNW was prepared by high intensity ultrasonication of CMF. 0.4g of as received CMF were immersed in 200 ml of distilled water (0.2w/v%) in a beaker 70 mm in diameter and 250 ml in volume at a temperature (T) of 25 ºC for 5min prior to being subjected to the ultrasonic treatment. Then, the HIU probe was immersed into the solution symmetrically aligned inside the beaker (without cooling bath) at a distance from the tip of the HIU probe to the bottom of the beaker of 7 mm.

Hydrogels preparation

The gelatin nanocellulose hydrogels were synthesized by freeze-thawing technique employing gum Arabic as crosslinking agent, according to the procedure reported in previous own works [19]. In brief, 10 % m/v of gelatin and 15 % w/w (refer to gelatin mass) of gum Arabic were dissolved in 100 mL in distilled water. This was maintained at 6°C during 24 h. After this time, the temperature of thermostatic bath rises to 50°C. Afterwards, a certain amount of nanocellulose (refer to gelatin and GA mass) was dissolved in 10 mL of distilled water and sonicated during 2 h. Then the temperature was raised to 60°C maintaining the sonication during 30 minutes. Thereafter, cellulose nanowhiskers suspension was incorporated to gelatin/gum Arabic solution maintaining under stirring during 30 minutes at 50°C. Finally, varied volumes of solution were filled in disposable molds allowing the gel formation at room temperature. The hydrogels were named as HGNC*x*, where *x* denotes the concentration (wt%.) of nanocellulose respect to gelatin and gum Arabic dry mass. Three different hydrogel were synthetized with 1, 2 and 5%wt NC. The Scheme 1 illustrates the pathways to obtain the hydrogels loaded NC.

Journal Pre-proof

A similar procedure was followed omitting the NC incorporation, obtaining raw GEL hydrogels (HG) that were taken as reference.

Scheme 1.Pathways to obtain different G10NC

Characterization techniques

FTIR spectroscopy

Fourier transforms infrared spectroscopy (FTIR) of hydrogels was recorder on a Thermo Scientific Nicolet iS50 FT-IR, modulo NIR: Thermo Scientific Nicolet iS50 NIR module with Integrating Sphere in the frequency range 4000-400 cm^{-1}.The ATR spectra were collected in a Thermo Scientific Nicolet 6700 spectrometer, with a resolution of 4 cm-1. 32 scans were performed over each sample from 600 to 4000 cm-1, the ATR (Attenuated Total Reflectance) accessory was utilized to perform the measurements.

Scanning electronic microscopy

The surface morphology of hydrogel was examined with a LEO EVO 40-XVP scanning electron microscope (SEM). The specimens of each hydrogel were swollen in distilled water, frozen, lyophilized and then fractured. All the samples were coated with gold before testing.

The morphology of cellulose nanowhiskers was analyzed by FESEM micrographs with a scanning electron microscope Supra55 microscope, Zeiss (Germany), with an acceleration voltage of 3 kV. Prior to the observation, the surfaces were sputter-coated with a gold layer to avoid charging under the electron beam.

Rheology assays

Rheological measurements were carried out using an Anton Paar Physica MCR 301 rheometer. Specimens of circular cross-section (25 mm diameter and 2 mm thickness), were tested using small amplitude oscillatory shear flow between parallel plates under nitrogen atmosphere. The elastic (G´) and the viscous (G´´) moduli were measured at 20 °C in a frequency range between 0.1 and 100 1/s with a 0.1% of strain. Besides

Journal Pre-proof

temperature sweeps were carried out from -60 ºC to 30 ºC, with heating rate of 5ºC/min. The elastic and viscous moduli were recorder as a function of temperature.

Thermal properties

Thermogravimetric measurements (TGA) of hydrogel matrix and gelatin/cellulose nanowhiskers hydrogels were performed by using a Shimadzu TGA-50 instrument. Tests were run from 20 °C to 500 °C at a heating rate of 10 °C/min under N_2 atmosphere.

Swelling assays

Swelling assays were performed in distilled water at room temperature. In this regard, air-dried cross section of hydrogels was weighted in the dry state. The samples were left swelling in both media in a closed vessel. The excess of water of each sample was removed with a filter paper before weighing. The increase in water uptake was determined at fixed time until the swelling equilibrium was reached. The swelling equilibrium degree was determined as:

$$SD(\%) = ((Wf - Wi) \div Wi) \times 100 \quad (1)$$

Determination of gel fraction

The gel fraction (GF%) was determined by weighting an hydrogel sample, previously dried in an oven at 37 ºC during 48hs (Mi). After this period of time the sample was immersed in distilled water during 1 to 4 days, depending on the kind of gel. Then, the sample was dried at 37 ºC until constant weight (Mf). The GF% was calculated as follows:

$$GF\% = (Mf/Mi) * 100 \quad (2)$$

The GF% was determined for HG matrix and HGNC.

Journal Pre-proof

Solubility assays

Solubility assays were performed by incubating the hydrogels in 100mL of distilled water (pH=5.5-6) at room temperature by measuring the mass lost after a period of 144hs. Therefore the partial solubilisation is expressed as %of mass lost by considering the initial(Mi)and final (Mf) dry weight of the HGs, according to equation (3). The chosen time was based on the time required to complete HG dissolution.

$$\text{Solubility\%} = (Mi - Mf/Mi) * 100 \qquad (3)$$

To further support and confirm gravimetric data, UV-visible spectroscopic analysis was performed using a UV visible spectrophotometer Agilent 8473 with diodes arrangement. Homogeneous aliquots of supernatant (4mL) were withdrawn at prefixed periods of times during HGs incubation in distilled water. UV visible spectra were recorded measuring the absorbance at 280nm. The same procedure was followed by incubating the raw polymers (GEL, GA and NC). The goal was to determine variations in the turbidity of the solution as a function of the incubation time as a qualitative measurement of the partial HG dissolution.

Lidocaine loading and release kinetics

The hydrogel containing 2% w/w of cellulose nanowhiskers (HGNC2) was selected for lidocaine incorporation. The selection was based on its physicochemical characteristics, as it will detail in the Results section. The procedure of LID incorporation involved the methodology described below for hydrogel synthesis, adding the drug with cellulose nanowhiskers and placed under vigorous stirring during 1h. The mixture was then transferred onto appropriate molds and allowed to dry at room temperature for 24 h.

Journal Pre-proof

Hydrogel containing 2% w/w of hydrochloride lidocaine was synthetized, the selection of this drug concentration was made taking into account the concentration of lidocaine presented by commercial gels for the mentioned applications.

The described procedure was performed using the HG and HGNC.

The release kinetic of lidocaine from the hydrogel was performed in phosphate buffer (PBS, pH=6.8) and put in thermostatically controlled water bath at 37 ± 0.5 °C. Such experimental conditions were adopted from available literature referring to buccal drug delivery systems [20][21][22].

Results and discussion

Spectroscopic analysis

FTIR spectra were recorded in order to investigate possible structural changes in hydrogels as well as to verify the NC incorporation. The spectrum of HG matrix displays a broad absorption band in the region of 3800-3900 cm^{-1} associated to hydroxyl groups from gelatin and gum Arabic [23]. Whereas the bands located between 1650 and 2300 cm^{-1} may be ascribed to amide groups from gelatin protein structure [24].

The role of GA in the crosslinking process of gelatin matrix is ascribed to the electrostatic interaction between the protein and polisaccharide improving the gelation properties [23,25]**.** It is worth noting that the presence of GA is not straightforward evidenced by FTIR because of overlapping with those arising from gelatin functional groups [26].

The typical bands of NC almost overlap with those corresponding to the functional groups of HG. For instance, a broad band is found ranging from 3500-3200 cm^{-1} indicative of the stretching vibration of free –OH groups due to the hydrogen bonding in cellulose molecules. It is also observable a signal around 2870 cm^{-1} attributed to *sp3* C-H stretching vibration. A low intensity vibration band, at 1365 cm^{-1}, could be identified as the

Journal Pre-proof

characteristic bending vibration of C-H and C-O bonds within the aromatic rings of polysaccharide. Besides, an intense peak was observed at 1061 cm^{-1} due to the stretching vibration of C-O-C pyranose ring of cellulose molecules [27,28]**.**

Figure 1. FTIR spectra of gelatin hydrogel matrix, nanocellulose and gelatin-nanocellulose hydrogels.

The spectra corresponding to HG with increasing concentrations of NC do not show significant differences between the raw materials, i.e HG and NC. A combination of the bands observed in the spectra of both is evidenced confirming the NC presence in the HG matrix.

Morphological analysis

The results achieved by SEM analysis give light about the composite morphology as it is shown in Figure 2. In Fig 2a, the images of raw HG are shown (as example), whereas Fig.2b exhibits the FE SEM micrographies of nanocelluse fibers. The morphologies of the HGNC hydrogels originated from increasing NC concentrations are compared in Figure 2c. From the analysis of these figures, it is clear that hydrogels matrix exhibits a porous structure with hole size of already 100 μm. The images in Fig. 2b reveals the average sizes obtained using the Image Pro Plus software. The average diameter was 37.5±6.1 nm and the long was 240nm. The aspect ratio was l/d: 6.40.

The addition of NC generates a denser surface in the hydrogel where the pore seems to be more compact as NC content increases. The nanofibers of cellulose may be observed located in the holes of the porous matrix. It seems to be pulled out indicating certain lack of adhesion between nanocellulose and the biopolymeric matrix. Other authors reported similar observations [4]**.**

Journal Pre-proof

Figure 2a. SEM images of raw nanocellulose wiskers (NC) acquired with different magnifications.

Figure 2b. SEM images of hydrogel matrix (HG) acquired with different magnifications.

Figure 2c. SEM images of hydrogel loaded different NC concentrations: i-HGNC1; ii-HGNC2 and iii-HGNC5, acquired with different magnifications.

Thermogravimetric analysis, gel fraction and solubility assays

The Figure 3 shows the TGA curve of neat hydrogel, NC loaded hydrogels and cellulose nanowhiskers.

Sample	**HG**	**HGNC1**	**HGNC2**	**HGNC5**	**NC**
Degradation Temperature, T_p,	308	310	315	315	333

<Figure 3.TGA curves of HG and HGNC>

Table 1 Degradation temperature of HG matrix and HGNC gels.

Journal Pre-proof

Journal Pre-proof

(°C)					

As a first observation, the T_p for the nanocomposites with 1, 2 and 5wt% of cellulose nanowhiskers, reveals that thermal stability increases by about 2, 7 and 7 °C, respectively when compared with HG raw gelatin gel (see also Table 1). It is known that the reinforcing effect depended not only on the cellulose nanowhiskers reinforcement in the polymeric matrix, but also is influenced by the occurrence of intermolecular hydrogen bonding interactions between the cellulose nanowhiskers and the polymers (GEL and GA) [4]**.** In this case, the improvement in thermal stability is not markedly, suggesting the presence of the reinforcement but not the interactions between them [29].

The GF data concerning HG matrix and HGNC are displayed in Figures 4, demonstrating that the incorporation of NC leads to a decrease in the GF. The addition of NC during the gel formation (see Scheme 1) partially hinders the interactions between the gum Arabic and gelatin functional groups leading to a less crosslinked hydrogel structure.

Figure 4.Gel fraction of hidrogel matrix and those loaded with increasing amounts of nanocellulose

The gelation of the matrix hydrogel is ascribed to the occurrence of intermolecular interactions between the protein molecules and the OH from GA by electrostatic and mainly hydrogen bonding forces. The incorporation of NC occurred in a posterior stage, once the GA-Gelatin interactions were stablished. It is thought that NC locates in the holes of the hydrogel structure partially weakening the GA-gelatin interactions [4].

As it may be observed from the analysis of hydrogels microstructure by SEM (Figures 2a-c), the raw hydrogel matrix exhibits a highly porous network with smooth aperture walls. The NC addition leaded to a more compact structure exhibiting smaller holes. The increasing amount of NC added to the gelatin matrix leaded to a gradual decrease in pore

Journal Pre-proof

size .Other authors have achieved similar results in exploring the gelatin crosslinking by means of cellulose nanowhiskers. They argued that the presence of cellulose provides higher number of junction points allowing a better intermolecular association. These facts have an impact on the size, structure and distribution of pore [30–32]. Other contribution suggests that the inclusion of NC moieties on gelatin hydrogel matrix arise to a reduction in pore size improving the shape homogeneity [33].

Therefore, the data arising from the GF% may be justified in terms of the changes in the hydrogel structure and the occurrence of further interactions between the protein fraction of gelatine and the NC.

The solubility data in terms of gravimetric measurements are included in Table 2.

Table 2. Solubility of different HGs formulations expressed as % after 144hs.

Formulation	**Initial mass (mg)**	**Final mass (mg)**	**Solubility(%)**
HG	$0.0497 \pm 1.0x10^{-4}$	$0.00333 \pm 2.0x10^{-4}$	94.33 ± 1.8
HGNC1	$0.0544 \pm 2.1x10^{-4}$	$0.0149 \pm 5.8x10^{-5}$	72.64 ± 1.2
HGNC2	$0.0571 \pm 1.0x10^{-4}$	$0.0377 \pm 1.0x10^{-4}$	34.00 ± 1.0
HGNC5	$0.0575 \pm 1.7x10^{-4}$	$0.0167 \pm 2.2x10^{-4}$	70.90 ± 2.1

From data on the Table it is evident that the incorporation of 1 and 5% of NC slightly reduces the solubilization rate of the hydrogels. However the 2% concentration of NC ensures a later solubilization against the time in the evaluated period. These results are supported by those arising from UV-visible analysis measuring at 200nm. Spectra of different HGs as a function of time are shown in Figure 5 a-d and the ones corresponding to raw polymers (GEL, GA and NC) are included as Supplementary Material. From such

Journal Pre-proof

These results are supported by those arising from UV-visible analysis measuring at 280nm. Spectra of different HGs as a function of time are shown in Figure 5 a-d and the ones corresponding to raw polymers (GEL, GA and NC) are included as Supplementary Material. From such Figures it may observe gelatin leaching, evidenced by the signal at low wavelength (lower than 100nm in the far UV region) and the rise of the absorbance at 280nm that may be ascribed to the presence of particles in dispersion arising from the partial dissolution of polymeric moieties [34]. It is clear that this signal intensified at higher times. Comparing the UV-visible spectra of all the formulations, it is found that HCNC2 exhibited the lower absorbance values at 280nm at any explored time, suggesting a lower level of degradation/dissolution against the time. These findings are in accordance with the gravimetric data (%S).

<Figure 5.UV-visible spectra of supernatant of HG incubation in distilled water:a.HG,b.HGNC1; c.HGNC2 and d.HGNC5>

The evolution of the solubility rate as a function of the time has been further evaluated by testing this property at 30 and 60 minutes. The data have been included in Supplementary Material (Figure S3) and reveals that at shorter incubation times the formulation HGNC2 exhibits an almost constant mass loss. Even when this is higher than the values corresponding to the other HGNC formulations in the first 60min, the final mass loss is sensibly lower. This behavior may be ascribed to a rearrangement and network distribution of the NC moieties on the Gel matrix the different NC[2][35].

The effect of NC in the gelatin based matrix is ascribed to the possibility to the NC to establish already strong interactions with the gelatin and/or even the Arabic gum functional groups. The incorporation of 2% of NC seems to ensure an optimum relation between the available functional groups and the NC moieties. The lower the NC concentration (1%) is

Journal Pre-proof

not enough to promote efficient interaction with the active sites on the HG matrix. Whereas the higher concentration (5%) induces the NC agglomeration rendering nanocellulose moieties physically deposited on the HG matrix with poor interaction ability. A similar behavior has been found by other authors studying alike systems. For instance, Denhad *et.al* have investigated the inclusion of bacterial cellulose on chitosan based films. They have found solubility rates ranging from 26-57% and stated that solubility rate may be controlled by adjusting the amount of incorporated NC. Their achievements regarding the solubility have been consistent with data on water vapor permeability [36].

In another recent work, H.W. Kwak et al. have studied the effect of adding different proportions (%W/W) of NC derivatives (di-aldehyde cellulose nanocrystals, DCNCs) on gelatin/chitosan films. They have reported that when the amount of DCNCs reached 15%, related to gelatin, excellent compatibility was attained. Additionally, the gelatin film reinforced with 15% D-CNCs showed lower solubility than that containing 20% DCNCs because the unreacted D-CNCs that do not participate in the cross-linking process with gelatin could be leached out.

They explained these data considering that increasing DCNC amount above 20%, aggregation or agglomeration occurred. They further verified this observation by examining the reduction in the transmittance of the prepared films[37].

The mentioned contributions are in line with the research developed by Agustin et. Al., dealing with the fabrication of cellulose-nanocrystal-reinforced maize film. These authors found that a higher nanocellulose concentration resulted in the typical nanocellulose aggregation behavior during water evaporation. Furthermore, the unexpected mechanical weakening effect of composite films occurred due to nanofiller aggregation [38][39].

Journal Pre-proof

Several articles in open literature report that the incorporation of nanocellulose functions as reinforcement and enhancer of mechanical and thermal properties of gelatin hydrogel, however it is not a clear tendency for their effect on films/gels solubility [4,30,40]**.**

It is worth mention that in most of published contributions the NC was added at the initial stages in contact with gelatin solution .In the present work the NC was incorporated after the freeze step, once the hydrogel structure was almost formed by gelatin/GA macromolecules. Therefore, the difference in the effect caused by NC incorporation may be ascribed to the synthetic pathways followed to assess HGNC.

Rheological properties

The figure 6a shows the complex viscosity as a function of frequency for the HG matrix and the gels prepared by increasing concentrations of NC. The tests were conducted at 20ºC. As it can be seen the presence of nanocellulose in gelatin hydrogel matrix affects the viscosity of the composites. The differences observed in the viscosity reflect changes in the matrix intermolecular forces such as hydrogen bonding. The viscosity decreased with increasing shear rate in the HGNC independently of the concentration of the NC initially added to the formulation. This characteristic is typical of non-Newtonian behavior where the viscosity decreases under shear strain, named shear thinning [41]. Similar results were found by Wang et al. [4].

Figure 6a. Complex viscosity as function of frequency for matrix and HGNC hydrogels

The dynamic viscoelastic properties were explored in order to further investigate the influence of nanocellulose. Figure 6b shows the G` and G`` curves of gelatin hydrogel as

Journal Pre-proof

function of frequency. The G` magnitudes are larger than G`` over the entire frequency range (tanδ< 1). This behavior indicates that all materials have a gel-like behavior. It seems that employing low concentration of nanocellulose there was not influence on the elastic modulus, indicating that the nanocellulose particles could not be integrated into gelatin hydrogel matrix. Meanwhile, by using 5% of nanocellulose during the synthesis procedure, the G` increased over the entire frequency range suggesting that an increment on the stiffness of the hydrogel matrix occurs. This result may be considered as evidence that the nanocellulose is effectively integrated in the gelatin hydrogel matrix at this concentration. Hence, a NC concentration dependent behavior is detected. Ge et al. analyzed the influence of the addition of chitin whiskers in gelatin composites hydrogels in a recent publication devoted to the study of rheological behavior in similar materials [42]. In this work, the authors attributed the stiffness of gelatin hydrogel with chitin whiskers due to noncovalent interaction between gelatin matrix and chitin.

Figure 6b. Elastic and viscous modulus as function of frequency for gelatin matrix and HGNC hydrogels

The viscoelastic moduli curves obtained as a function of the temperature scanning test of hydrogel with different nanocellulose concentration and the corresponding to matrix hydrogel are presented in Figure 6c. It can be observed that elastic (G´) and viscous modulus (G´´) obtained within the range tested had higher values at lower temperatures than at comparatively higher temperatures. Besides, by increasing the temperature, all the hydrogels showed thermoreversible behaviors, and G´ and G´´ decreased upon heating. This thermo-reversible behavior may be ascribed to the different energy requirements for association and disassociation of junction zones of gelatin strands [43]. All the hydrogels maintained the gel structure since G´ exhibited higher values than G´´ in the temperature

Journal Pre-proof

range explored within this work. It can be observed that using higher concentrations of nanocellulose, 2 and 5%, led to higher viscoelastic moduli (G´ and G´´) when compared with the data corresponding to gelatin hydrogel matrix and also, with HGNC containing 1% of nanocellulose. This behavior could be attributed to the nature of interaction between gelatin matrix and nanocellulose and with the pathways involved in synthesis procedure. The gelation of gelatin is due to intermolecular interactions among protein molecules always includes electrostatic, hydrogen bonding as well as hydrophobic interactions [44]. Therefore, it may infer that a percolation threshold was reached when high nanocellulose concentrations are employed. Other authors, analyzing the mechanical reinforcement of gelatin hydrogel with nanofiber cellulose, obtained similar results [4].

Figure 6c. Temperature dependence of G` and G`` for gelatin matrix and HGNC hydrogels

Swelling behavior

Figure 7 shows the swelling behavior of raw HG matrix and HGNC in distilled water at room temperature as a function of the time. The water uptake of the matrix reached a maximum of 700%, maintaining the structure in the swollen state from almost 48 h. The NC incorporation leads to hydrogels exhibiting swollen equilibrium at 24h, maintaining their structure. The maximum swelling degree was higher (almost 600%) for HG containing lower NC nominal concentration (HGNC1 and NC2) whereas it reached already 500% for the HG with higher NC content (HGNC5)

It is important to highlight that the stability of gelatin-nanocellulose hydrogels in water was retained during almost 24 h, exceeding this time the hydrogels start to undergo disintegration. These results are in accordance with those previously discussed, since further confirm that the NC incorporated to the matrix would be located in the hydrogel pores hindering the diffusion of water molecules to the polymeric network.

Figure 7. Swelling of HG and HGNC with increasing NC concentrations

Journal Pre-proof

in water at room temperature

Loading and release of lidocaine from NC gelatin hydrogels

Hydrogel formulations yield relatively rapid drug release because of the high water content and large pore size [45]. Also, most of hydrogels are not injectable (except the ones in situ formed), hence the proposed pharmaceutical form of HGNC-LID is thought to be as patches directly applied on the injury region, such as some commercial devices [46]**.**

The loading of lidocaine was performed by encapsulation of the therapeutic agent during the preparation of the gelatin hydrogel, simultaneously with the incorporation of the NC moieties. This procedure is represented in the Scheme 2. It is worth mention that the formulation HGNC2 was selected to the LID loading because of its swelling properties and mainly its stability in distilled water. As it was discussed earlier this formulation ensured lower solubilization/degradation during incubation in DW during six days. This ability resulted interesting not only from the basic study of the interactions between the polymeric matrix and the drug, but also for future ex vivo or in vivo assays.

Journal Pre-proof

Scheme 2.Pathways to the LID loading on hydrogel matrix.

The concentration of the drug was chosen considering the proportions of lidocaine in major of commercial devices according to the therapeutic doses commonly required for buccal treatments **(9).**

The encapsulation of the drug on the HGNC matrix was qualitatively verified by FTIR-ATR spectroscopy. The spectrum of raw LID shows a complex number of signals ascribed to excipients and stabilizers added to the commercial drug used within this work, and it is

Journal Pre-proof

included in Supplementary Material. However benzene ring from LID produces the signal at about the 3030 cm^{-1} range. While the C=C may be found at the 1450-1600 cm^{-1} range as a strong band. A signal appearing in the 3000-3500 cm^{-1} range may be ascribed to the H-N-C=O amide group . A carboxylate group vibration may be detected as a signal in the 1630-1690 cm^{-1} range [47].The N attached to 3 carbons is a tertiary amine, but since it is not connected to any H directly, it does not produce a signal in the 3200-3500 cm^{-1} range like the other amines do. It produces the signal in the 1020-1360 cm^{-1} range instead. All described signals are evidenced in the spectrum of HGNC2 loaded LID included in Figure 8.

<Figure 8.ATR spectra of HGNC2 and HGNC2 loaded LID>

By comparing such spectrum with the corresponding to the raw HGNN2 the appearance of a shoulder in the region of ~3550cm^{-1} is detected. Besides slight shifts in the signals ascribed to C=O groups ~1660-1685cm^{-1} are observed. These minor differences between both spectra may be considered as evidences for the interactions between the polymeric moieties and the LID. Similar findings have been reported by other authors [48].

Release profiles

The most common anaesthetics, such as LID, share a common chemical structure composed of an hydrophobic aromatic fraction linked by an amide to a tertiary amine (with a pKa of 7–8; see Scheme 2). Therefore, LID under acidic conditions is typically hydrophilic [49]**.**

Examining the release profiles, included in Figures 9a and b, noticeably differences may be observed when LID is encapsulated in the HG matrix with respect to the drug loaded on HGNC hydrogel.

Journal Pre-proof

In Figure 9a the release of LID is characterized by a typical initial burst effect during the first 30min, followed by a gradual percentage of LID delivered until 120min where the equilibrium is reached. The release assays were conducted during 300min because after this time the gel began its degradation process hampering the reliable quantification of LID by UV-visible.

From Figure 9a it is possible to see that the release of the therapeutic agent is almost incomplete reaching a maximum percentage of about 55% with respect to the LID initially encapsulated on the hydrogel matrix.

The presence of NC in the HG matrix strongly affects the release profile. Although a roughly similar profile is observed during the first 30min (also characterized by a burst effect), the remainder LID is quickly and completely (100%) released during the next 120min.

These data coincide with the previously discussed concerning to the structural characterization of the gels, in terms of the swelling behavior, TGA, morphologic, gel fraction and solubility analysis. It is important to highlight that the release assays were performed in PBS buffer at pH 6.8 with high saline content. These media characteristics seriously affected the integrity of the hydrogel regarding the stability/solubility against the time.

It may infer that strong electrostatic interactions operate between the GEL-GA matrix and the LID, leading to a slow and incomplete release (Fig. 9a).In the HGNC matrix such electrostatic interactions are partially blocked by the presence of NC affecting GEL-GA available functional groups. However, it is evident that both release profiles (Fig.9a and 9.B) are almost similar during the first 30min of assay. This fact suggests that at least 25% of the loaded LID remains free (unbounded) in the polymeric network displaying similar delivery dynamic than in the case of raw HGNC[20] . The further LID release was mainly

Journal Pre-proof

governed by the movement of the drug from the gel network. This fact may justify the observed differences [50].

The inclusion of NC on HG matrix weakens the hydrogel structure, as was earlier discussed, and further inhibits the LID-GEL-GA interactions. This enables the quick release of the drug during the first 120min. Release times ranging from minutes to scarce hours have been reported in open literature by other authors working with films and gels of different composition [16]. For instance, Medhi et al reported the complete release of LID from polymeric microparticles in almost 1hour using distilled water as release media. They justified that the release was not in the seconds range then it may not be considered as a fast release system. They also argued that this behavior might be dose dependent [51].

Figure 9a-Release profile of LID from HG matrix

9b-Release profile of LID from HGNC matrix.

To predict the delivery of lidocaine from the prepared hydrogels a fundamental understanding of the mechanisms controlling its release is necessary. The applied mathematical models have been selected on the basis of published articles regarding DDS using different polymeric matrixes as micro/nanoparticulate devices as well as hydrogels [52–55].

The experimental release data were fitted to Equations (1) to (4) by plotting the following:

- cumulative percentage drug release vs time (zero-order kinetic model);
- log cumulative percentage drug remaining vs time (first-order kinetic model);
- cumulative percentage drug release vs square root of time (Higuchi model);

Journal Pre-proof

- log cumulative percentage drug release vs log time (Korsmeyer model);

The results of these fittings are given in Table 3, expressed in terms of the correlation factor (*r*2). Data on the Table 3 reveals that the best model was the First order for any of the hydrogels evaluated. Other authors haver reported similar findings studying the release of oxalilplatin from gelatine based hydrogels as drug delivery systems.

They suggested that the release kinetic of hydrophilic drugs, such as lidocaine, involves the entry of dissolution medium via micro channels into the polymeric network, dissolution of the drug in this medium followed by subsequent migration of these small packets containing the dissolved drug to the surface [56]**.**

From the data in Table 3, it is clear that the values of *r*2 corresponding to the HG LID shows a greater deviation from1, than the *r*2 values were corresponding to HGNC-LID. This may be related to complex interaction between the polymeric moieties and the drug influenced by the presence of NC.

Table 3. Results of kinetic model fitting in terms of correlation coefficients, r2 for HG and HGNC loaded LID.

Mathematical Model	HG-LID	HGNC-LID
	r^2	r^2
Cero order	0,5001	0.7698
First order	0.9014	0.9958
Higuchi	0.7709	0.9356
Korsmeyer	0.8381	0.9224

The drug release mechanism from these systems is generally described by calculating the value of ‘n’ through the Korsmeyer–Peppas model [50,57]. In both formulations (HGLID

Journal Pre-proof

and HGNC LID) the value of n was lower than 0.45, indicating that fickian diffusion is the dominant mechanism of release [56].

From this result it is possible infer that the hydrogel erosion promotes the LID release from the hydrogels network. Lidocaine releases from the gel bulk both through diffusion out of the formulation and as a result of gel erosion [57].

As it was earlier commented, the articles in open literature reporting the use of different kinds of delivery systems to the administration of LID are numerous; however those devoted to the formulation of buccal dispositive to dentistry treatments are limited.

Susuki et. Al synthesized a sustained-release lidocaine sheet (SRLS) using biodegradable polymers (PLGA) and previously demonstrated its safety and long-term analgesic effect in the normal mucous membrane of healthy human volunteers [58]. In a more recent contribution (2018) , the same authors developed a clinical study to evaluate the efficacy, safety, and appropriate dose of the SRLS for pain following tooth extraction [58]. They compared the efficacy of raw LID, raw PLGA (biopolymers composing the sheets) and different masses of SLRS, I.e 100, 200 and 400mg loaded with 40, 80, 160mg of LID, respectively in the shape of squares of 2 cmx2 cm. The application after the tooth extraction revealed that PLGA Control group showed the strongest pain, probably caused by the filling pressure at the socket itself. In that regard, in the SRLS 100 mg group, the released lidocaine may have suppressed the pain derived from the filling pressure. The SRLS 100 mg resulted in the most suitable formulation because of analgesia, by the released lidocaine, and the negative influence from the filling pressure seemed to be balanced [58].

In another earlier research moldable films called “Denticaps” were formulated by combining polymeric moieties: eudragit L 100-55, carbopol 971 P, gum karaya powder, ethyl cellulose and another with corn zein, carbopol 934 P, gum karaya, poloxamer 407,

Journal Pre-proof

ethyl cellulose and loaded with 10%w/w of LID. To evaluate the in vivo release study, 10 adult human volunteers (both male and female) were administrated with Denticaps in buccal cavity over tooth surface and asked to notice the local anesthetic effect of Lidocaine hydrochloride over a time period of 8- 12 h. The goal was to verify the sustained local effect of the drug from the designed polymeric film. They found that the Denticap onset of action of Lidocaine hydrochloride in upper jaw and lower jaw were between 3 and 1 minutes, depending on the film formulation. Whereas Duration of action of Lidocaine hydrochloride in Denticap was 125 and 90 minutes for application on the tooth surface at upper jaw and lower jaw, respectively. Those dispositive contained a ratio 1:10 from LID to the total polymeric mass, and the total weight of the Denticap was 500mg. That means that the LID administrated was around 50mg [59].

DentiPatch' lidocaine transoral delivery system (Noven Pharmaceuticals, Miami, Fla), is one of the commercial formulation that may be compared with the HGs proposed within this work. DentiPatch has been approved by the United States Food and Drug Administration (FDA) for clinical use in the production of mild, topical anesthesia of mucosal membranes in the mouth. It contains almost 46.1 mg of lidocaine. The way of patches administration is by helding firmly on the tissue for 30 seconds. The patch was then allowed to remain adhered to the area for a period of 5 minutes. The scientific reports stated that this time-doses purportedly maximizes the effect of lidocaine diffusing into a localized mucosal site to reduce the pain associated with injections [60].

When considering the data arising from HGs proposed within our work, it is found that the loaded LID reached almost 20 mg LID/g HG. Therefore, extrapolaiting to the potential implementation conditions of HGs, it is possible consider a patch of about 5g (4cm^2 aprox.) where the dose of LID would be around 100mg. According to the kinetic data included in Figure 9b; 30% of the LID was released after 5min of incubation; this percentage represents near 30mg of drug. This quantity is near the 46.1mg informed by applying the

Journal Pre-proof

commercial formulation in the same period of time. These data may be considered as an estimation of the expected behaviour of HGNC-LID applied as patches. This could be taken as an initial approach to assess the corresponding in vivo-ex vivo experiments.

Concluding remarks

Gelatin –gum Arabic hydrogels modified with have been successfully prepared. The incorporation of nanocellulose whiskers played a key role, allowing the control over solubility and swelling properties.

The GF demonstrated to decrease as the amount of added NC increased. These data are in line with those arising from characterization, i.e. FTIR, SEM, TG and rheology.

Solubility and swelling data revealed HGNC2 as the better formulation to the loading of LID.

The encapsulation of LID, as model drug intended for dental treatments, was successfully achieved as demonstrate FTIR results. The release kinetic and mechanism strongly depended on the hydrogel structure showing great differences between HG and HGNC matrix.

Besides HGNC-LID contains the amount of drug commonly found in most commercial formulations. Therefore these gelatine based hydrogels may be considered as viable raw materials for the fabrication of dental patches destined to the local administration of anahestesia in buccal treatments. This contribution constituted the initial stage to advance in further in vivo –ex vivo assays.

It is worth mention that the LID load was taken as example, hence this platform may be adapted to the administration of several therapeutic agents destined to buccal treatments.

Acknowledgements

Journal Pre-proof

The authors acknowledge the financial support of CONICET, ANPCyT National University of Mar del Plata and National University of South.

References

[1] J.S. Gonzalez, C. Mijangos, R. Hernandez, Polysaccharide Coating of Gelatin Gels for Controlled BSA Release, Polymers (Basel). 11 (2019) 702. https://doi.org/10.3390/polym11040702.

[2] G. Mondragon, C. Peña-rodriguez, A. González, A. Eceiza, A. Arbelaiz, Bionanocomposites based on gelatin matrix and nanocellulose, Eur. Polym. J. 62 (2015) 1–9. https://doi.org/10.1016/j.eurpolymj.2014.11.003.

[3] A. Gupta, M. Kowalczuk, W. Heaselgrave, S.T. Britland, C. Martin, I. Radecka, The production and application of hydrogels for wound management: A review, Eur. Polym. J. 111 (2019) 134–151. https://doi.org/10.1016/j.eurpolymj.2018.12.019.

[4] W. Wang, X. Zhang, A. Teng, A. Liu, Mechanical reinforcement of gelatin hydrogel with nanofiber cellulose as a function of percolation concentration, Int. J. Biol. Macromol. 103 (2017) 226–233. https://doi.org/10.1016/j.ijbiomac.2017.05.027.

[5] C. Alamanos, P. Raab, A. Gamulescu, M. Behr, Ophthalmologic complications after administration of local anesthesia in dentistry: A systematic review, Oral Surg. Oral Med. Oral Pathol. Oral Radiol. 121 (2016) e39–e50. https://doi.org/10.1016/j.oooo.2015.10.023.

[6] K.K. Park, V.R. Sharon, A review of local anesthetics: Minimizing risk and side effects in cutaneous surgery, Dermatologic Surg. 43 (2017) 173–187. https://doi.org/10.1097/DSS.0000000000000887.

[7] B. Wang, S. Wang, Q. Zhang, Y. Deng, X. Li, L. Peng, X. Zuo, M. Piao, X. Kuang, S. Sheng, Y. Yu, Recent advances in polymer-based drug delivery systems for local anesthetics, Acta Biomater. (2019) 1–13. https://doi.org/10.1016/j.actbio.2019.05.044.

[8] L. Kearney, D. Whelan, B.D. O'Donnell, A.J.P. Clover, Novel methods of local anesthetic delivery in the perioperative and postoperative setting—potential for fibrin hydrogel delivery, J. Clin. Anesth. 35 (2016) 246–252. https://doi.org/10.1016/j.jclinane.2016.07.033.

[9] M. Khanal, S. V. Gohil, E. Kuyinu, H.M. Kan, B.E. Knight, K.M. Baumbauer, K.W.H. Lo, J. Walker, C.T. Laurencin, L.S. Nair, Injectable nanocomposite analgesic

Journal Pre-proof

delivery system for musculoskeletal pain management, Acta Biomater. 74 (2018) 280–290. https://doi.org/10.1016/j.actbio.2018.05.038.

[10] X. Liu, Q. Zhao, Long-term anesthetic analgesic effects: Comparison of tetracaine loaded polymeric nanoparticles, solid lipid nanoparticles, and nanostructured lipid carriers in vitro and in vivo, Biomed. Pharmacother. 117 (2019) 109057. https://doi.org/10.1016/j.biopha.2019.109057.

[11] F.L. Esteban Florez, Y. Pathak, C. Preuss, Chapter 24 - Orally delivered nanoparticle drug-delivery systems for dental applications and their systemic toxicity, Elsevier Inc., 2019. https://doi.org/https://doi.org/10.1016/B978-0-12-815886-9.00024-3.

[12] A. Bernkop-Schnürch, G. Walker, Multifunctional matrices for oral peptide delivery, Crit. Rev. Ther. Drug Carrier Syst. 18 (2001) 459–501.

[13] C.M. Santamaria, A. Woodruff, R. Yang, D.S. Kohane, Drug delivery systems for prolonged duration local anesthesia, Mater. Today. 20 (2017) 22–31. https://doi.org/10.1016/j.mattod.2016.11.019.

[14] S. Singh, P.K. Sharma, N. Kumar, R. Dudhe, DESIGN, DEVELOPMENT AND EVALUATION OF MUCOADHESIVE PATCHES OF REPAGLINIDE FOR BUCCAL DELIVERY, Int. J. Pharmacy&Technology IJPT. 2 (2010) 259–580.

[15] M. Bågesund, P. Tabrizi, Lidocaine 20% patch vs lidocaine 5% gel for topical anaesthesia of oral mucosa, Int. J. Paediatr. Dent. 18 (2008) 452–460. https://doi.org/10.1111/j.1365-263X.2007.00910.x.

[16] C. Cavallari, A. Fini, F. Ospitali, Mucoadhesive multiparticulate patch for the intrabuccal controlled delivery of lidocaine, Eur. J. Pharm. Biopharm. 83 (2013) 405–414. https://doi.org/10.1016/j.ejpb.2012.10.004.

[17] A. Nayak, D.B. Das, G.T. Vladisavljević, Microneedle-assisted permeation of lidocaine carboxymethylcellulose with gelatine Co-polymer hydrogel, Pharm. Res. 31 (2014) 1170–1184. https://doi.org/10.1007/s11095-013-1240-z.

[18] M.E. Bracone, Optimization Of Acid Hydrolysis Process For The Preparation Cellulose Nanofibrils, Adv. Mater. Lett. 10 (2019) 499–507. https://doi.org/10.5185/amlett.2019.2182.

[19] M.F. Horst, M.D. Ninago, V. Lassalle, Magnetically responsive gels based on crosslinked gelatin: An overview on the synthesis, properties, and their potential in water remediation, Int. J. Polym. Mater. Polym. Biomater. 0 (2017) 1–13. https://doi.org/10.1080/00914037.2017.1362640.

Journal Pre-proof

[20] A. Rohani Shirvan, A. Bashari, N. Hemmatinejad, New insight into the fabrication of smart mucoadhesive buccal patches as a novel controlled-drug delivery system, Eur. Polym. J. 119 (2019) 541–550. https://doi.org/10.1016/j.eurpolymj.2019.07.010.

[21] J. Xu, S. Strandman, J.X.X. Zhu, J. Barralet, M. Cerruti, Genipin-crosslinked catechol-chitosan mucoadhesive hydrogels for buccal drug delivery, Biomaterials. 37 (2015) 395–404. https://doi.org/10.1016/j.biomaterials.2014.10.024.

[22] M.A. Akl, M.A. Hady, O.M. Sayed, Buccal mucosal accumulation of dapoxetine using supersaturation, co-solvent and permeation enhancing polymer strategy, J. Drug Deliv. Sci. Technol. 55 (2020) 101411. https://doi.org/10.1016/j.jddst.2019.101411.

[23] M. Anvari, C.H. Pan, W.B. Yoon, D. Chung, Characterization of fish gelatin-gum arabic complex coacervates as influenced by phase separation temperature, Int. J. Biol. Macromol. 79 (2015) 894–902. https://doi.org/10.1016/j.ijbiomac.2015.06.004.

[24] N. Johar, I. Ahmad, A. Dufresne, Extraction, preparation and characterization of cellulose fibres and nanocrystals from rice husk, Ind. Crops Prod. 37 (2012) 93–99. https://doi.org/10.1016/j.indcrop.2011.12.016.

[25] M.F. Horst, D.F. Coral, M.B. Fernández van Raap, M. Alvarez, V. Lassalle, Hybrid nanomaterials based on gum Arabic and magnetite for hyperthermia treatments, Mater. Sci. Eng. C. 74 (2016) 443–450. https://doi.org/10.1016/j.msec.2016.12.035.

[26] P.R. Sarika, N.R. James, Preparation and characterisation of gelatin–gum arabic aldehyde nanogels via inverse miniemulsion technique, Int. J. Biol. Macromol. 76 (2015) 181–187. https://doi.org/10.1016/j.ijbiomac.2015.02.038.

[27] T. Abitbol, A. Rivkin, Y. Cao, Y. Nevo, E. Abraham, T. Ben-shalom, S. Lapidot, O. Shoseyov, Nanocellulose , a tiny fiber with huge applications, Curr. Opin. Biotechnol. 39 (2016) 76–88. https://doi.org/10.1016/j.copbio.2016.01.002.

[28] S.Y. Ooi, I. Ahmad, M.C.I.M. Amin, Cellulose nanocrystals extracted from rice husks as a reinforcing material in gelatin hydrogels for use in controlled drug delivery systems, Ind. Crops Prod. 93 (2016) 227–234. https://doi.org/10.1016/j.indcrop.2015.11.082.

[29] S. Maiti, J. Jayaramudu, K. Das, S.M. Reddy, R. Sadiku, S.S. Ray, D. Liu, Preparation and characterization of nano-cellulose with new shape from different precursor, Carbohydr. Polym. 98 (2013) 562–567. https://doi.org/10.1016/j.carbpol.2013.06.029.

[30] R. Dash, M. Foston, A.J. Ragauskas, Improving the mechanical and thermal

Journal Pre-proof

properties of gelatin hydrogels cross-linked by cellulose nanowhiskers, Carbohydr. Polym. 91 (2013) 638–645. https://doi.org/10.1016/j.carbpol.2012.08.080.

[31] T. Huang, Z. cai Tu, H. Wang, X. Shangguan, L. Zhang, N. hai Zhang, N. Bansal, Pectin and enzyme complex modified fish scales gelatin: Rheological behavior, gel properties and nanostructure, Carbohydr. Polym. 156 (2017) 294–302. https://doi.org/10.1016/j.carbpol.2016.09.040.

[32] O.S. Yin, I. Ahmad, M.C.I.M. Amin, Synthesis of chemical cross-linked gelatin hydrogel reinforced with cellulose nanocrystals (CNC), in: AIP Conf. Proc., 2014: pp. 375–380. https://doi.org/10.1063/1.4895226.

[33] S. Ge, Q. Liu, M. Li, J. Liu, H. Lu, F. Li, S. Zhang, Q. Sun, L. Xiong, Enhanced mechanical properties and gelling ability of gelatin hydrogels reinforced with chitin whiskers, Food Hydrocoll. 75 (2018) 1–12. https://doi.org/10.1016/j.foodhyd.2017.09.023.

[34] H.P. Lim, K.W. Ho, C.K. Surjit Singh, C.W. Ooi, B.T. Tey, E.S. Chan, Pickering emulsion hydrogel as a promising food delivery system: Synergistic effects of chitosan Pickering emulsifier and alginate matrix on hydrogel stability and emulsion delivery, Food Hydrocoll. 103 (2020) 105659. https://doi.org/10.1016/j.foodhyd.2020.105659.

[35] A. Al-Sabah, S.E.A. Burnell, I.N. Simoes, Z. Jessop, N. Badiei, E. Blain, I.S. Whitaker, Structural and mechanical characterization of crosslinked and sterilised nanocellulose-based hydrogels for cartilage tissue engineering, Carbohydr. Polym. 212 (2019) 242–251. https://doi.org/10.1016/j.carbpol.2019.02.057.

[36] D. Dehnad, Z. Emam-Djomeh, H. Mirzaei, S.-M. Jafari, S. Dadashi, Optimization of physical and mechanical properties for chitosan–nanocellulose biocomposites, Carbohydr. Polym. 105 (2014) 222–228. https://doi.org/10.1016/j.carbpol.2014.01.094.

[37] H.W. Kwak, H. Lee, S. Park, M.E. Lee, H.J. Jin, Chemical and physical reinforcement of hydrophilic gelatin film with di-aldehyde nanocellulose, Int. J. Biol. Macromol. 146 (2020) 332–342. https://doi.org/10.1016/j.ijbiomac.2019.12.254.

[38] M.B. Agustin, B. Ahmmad, E.R.P. De Leon, J.L. Buenaobra, J.R. Salazar, F. Hirose, Starch-based biocomposite films reinforced with cellulose nanocrystals from garlic stalks, Polym. Compos. 34 (2013) 1325–1332. https://doi.org/10.1002/pc.22546.

[39] Y. Qin, S. Zhang, J. Yu, J. Yang, L. Xiong, Q. Sun, Effects of chitin nano-whiskers on the antibacterial and physicochemical properties of maize starch films,

Journal Pre-proof

Carbohydr. Polym. 147 (2016) 372–378. https://doi.org/10.1016/j.carbpol.2016.03.095.

[40] N. Naseri, B. Deepa, A.P. Mathew, K. Oksman, L. Girandon, Nanocellulose-Based Interpenetrating Polymer Network (IPN) Hydrogels for Cartilage Applications, Biomacromolecules. 17 (2016) 3714–3723. https://doi.org/10.1021/acs.biomac.6b01243.

[41] A. Rafe, S.M.A. Razavi, Scaling law, fractal analysis and rheological characteristics of physical gels cross-linked with sodium trimetaphosphate, Food Hydrocoll. 62 (2017) 58–65. https://doi.org/10.1016/j.foodhyd.2016.07.021.

[42] I.C.F. Moraes, R.A. Carvalho, A.M.Q.B. Bittante, J. Solorza-Feria, P.J.A. Sobral, Film forming solutions based on gelatin and poly(vinyl alcohol) blends: Thermal and rheological characterizations, J. Food Eng. 95 (2009) 588–596. https://doi.org/10.1016/j.jfoodeng.2009.06.023.

[43] T.R. Hoare, D.S. Kohane, Hydrogels in drug delivery: Progress and challenges, Polymer (Guildf). 49 (2008) 1993–2007. https://doi.org/10.1016/j.polymer.2008.01.027.

[44] A. Leopold, S. Wilson, J.S. Weaver, A.M. Moursi, Pharmacokinetics of lidocaine delivered from a transmucosal patch in children., Anesth. Prog. 49 (2002) 82–7.

[45] H.A. Mclure, A.P. Rubin, Review of local anaesthetic agents, Minerva Anestesiol. 71 (2005) 59–74.

[46] D. Svirskis, K. Chandramouli, P. Bhusal, Z. Wu, J. Alphonso, J. Chow, D. Patel, R. Ramakrishna, S.J. Yeo, R. Stowers, A. Hill, J. Munro, S.W. Young, M. Sharma, Injectable thermosensitive gelling delivery system for the sustained release of lidocaine, Ther. Deliv. 7 (2016) 359–368. https://doi.org/10.4155/tde-2016-0014.

[47] Y. Wei, M.P. Nedley, S.B. Bhaduri, X. Bredzinski, S.H.S. Boddu, Masking the Bitter Taste of Injectable Lidocaine HCl Formulation for Dental Procedures, AAPS PharmSciTech. 16 (2015) 455–465. https://doi.org/10.1208/s12249-014-0239-z.

[48] Y. Umeda, T. Fukami, T. Furuishi, T. Suzuki, M. Makimura, K. Tomono, Molecular complex consisting of two typical external medicines: Intermolecular interaction between indomethacin and lidocaine, Chem. Pharm. Bull. 55 (2007) 832–836. https://doi.org/10.1248/cpb.55.832.

[49] D.Y. Arifin, L.Y. Lee, C.H. Wang, Mathematical modeling and simulation of drug release from microspheres: Implications to drug delivery systems, Adv. Drug Deliv. Rev. 58 (2006) 1274–1325. https://doi.org/10.1016/j.addr.2006.09.007.

Journal Pre-proof

[50] J. Siepmann, N.A. Peppas, Modeling of drug release from delivery systems based on hydroxypropyl methylcellulose (HPMC), Adv. Drug Deliv. Rev. 64 (2012) 163–174. https://doi.org/10.1016/j.addr.2012.09.028.

[51] P. Medhi, O. Olatunji, A. Nayak, C.T. Uppuluri, R.T. Olsson, B.N. Nalluri, D.B. Das, Lidocaine-loaded fish scale-nanocellulose biopolymer composite microneedles, AAPS PharmSciTech. 18 (2017) 1488–1494. https://doi.org/10.1208/s12249-017-0758-5.

[52] V. Lassalle, M.L. Ferreira, PLGA based drug delivery systems (DDS) for the sustained release of insulin : insight into the protein / polyester interactions and the insulin release behavior Ver onica, (2010) 1588–1596. https://doi.org/10.1002/jctb.2470.

[53] G. Spadaro, C. Dispenza, G. Giammona, G. Pitarresi, G. Cavallaro, Cytarabine release from a a,b-poly (N- hydroxyethyl) -DL-aspartamide matrices cross-linked through y-radiation, 17 (1996) 953–958.

[54] K. Ullah, S. Ali Khan, G. Murtaza, M. Sohail, Azizullah, A. Manan, A. Afzal, Gelatin-based hydrogels as potential biomaterials for colonic delivery of oxaliplatin, Int. J. Pharm. 556 (2019) 236–245. https://doi.org/10.1016/j.ijpharm.2018.12.020.

[55] N.A. Peppas, SOLUTE AND PENETRANT DIFFUSION IN SWELLABLE POLYMERS. IX. THE MECHANISMS OF DRUG RELEASE FROM pH-SENSITIVE SWELLING- CONTROLLED SYSTEMS, J. Control. Release. 8 (1989) 267–274.

[56] R.W. Korsmeyer, E. Von Meerwall, N.A. Peppas, Solute and penetrant diffusion in swellable polymers. II. Verification of theoretical models, J. Polym. Sci. Part B Polym. Phys. 24 (1986) 409–434. https://doi.org/10.1002/polb.1986.090240215.

[57] E.J. Ricci, M.V.L.B. Bentley, M. Farah, R.E.S. Bretas, J.M. Marchetti, Rheological characterization of Poloxamer 407 lidocaine hydrochloride gels, Eur. J. Pharm. Sci. 17 (2002) 161–167. https://doi.org/10.1016/S0928-0987(02)00166-5.

[58] T. Suzuki, K. Kosugi, T. Suto, M. Tobe, Y. Tabata, S. Yokoo, S. Saito, Sustained-release lidocaine sheet for pain following tooth extraction: A randomized, single-blind, dose-response, controlled, clinical study of efficacy and safety, PLoS One. 13 (2018) e0200059. https://doi.org/10.1371/journal.pone.0200059.

[59] B.S. and B.M. Gopa Roy, Soma Ghosh, In vivo evaluation and the stability study of the formulation “Denticap” intended for local application to relieve dental pain, Int J Pharm Sci Tech. 3 (2009) 18–24.

[60] T. Andrea Leopold, DDS, MS,*t Stephen Wilson, DMD, MA, PhD,*t Joel S. Weaver,

Journal Pre-proof

DDS, PhD, P. and Amr M. Moursi, DDS, Pharmacokinetics of Lidocaine Delivered From a Transmucosal Patch in Children, Anesth Prog. 49 (2002) 82–87.

Figure captions

Scheme 1.Pathways to obtain different G10NC

Figure 1. FTIR spectra of gelatin hydrogel matrix, nanocellulose and gelatin-nanocellulose hydrogels.

Figure 2a. SEM images of raw nanocellulose whiskers (NC) acquired with different magnifications.; Figure 2b. SEM images of hydrogel matrix (HG) acquired with different magnifications; Figure 2c. SEM images of hydrogel loaded different NC concentrations: i-HGNC1; ii-HGNC2 and iii-HGNC5, acquired with different magnifications.

Figure 3.TGA curves of HG and HGNC

Figure 4.Gel fraction of hidrogel matrix and those loaded with increasing amounts of nanocellulose.

Figure 5. UV-visible spectra of supernatant of HG incubation in distilled water:a.HG,b.HGNC1; c.HGNC2 and d.HGNC5.

Figure 6a. Complex viscosity as function of frequency for matrix and HGNC hydrogels Figure 6b. Elastic and viscous modulus as function of frequency for gelatin matrix and HGNC hydrogels ;Figure 6c. Temperature dependence of G` and G`` for gelatin matrix and HGNC hydrogels

Journal Pre-proof

Figure 7. Swelling of HG and HGNC with increasing NC concentrations

in water at room temperature.

Figure 8.ATR spectra of HGNC2 and HGNC2loaded LID

Scheme 2. Pathways to the LID loading on hydrogel matrix.

Figure 9a-Release profile of LID from HG matrix

9b-Release profile of LID from HGNC matrix.

Table Captions

Table 1 Degradation temperature of HG matrix and HGNC gels.

Table 2. Solubility of different HGs formulations expressed as % after 144hs.

Table 3. Results of kinetic model fitting in terms of correlation coefficients, r2 for HG and HGNC loaded LID.

Journal Pre-proof

Journal Pre-proof

'Declarations of interest: none'.

Journal Pre-proof